Am J Cancer Res 2023;13(5):2087-2103
www.ajcr.us /ISSN:2156-6976/ajcr0148667

Original Article

Decoding the biological properties and transcriptomic landscapes of human natural killer cells derived from bone marrow and umbilical cord blood

Baoguo Xie[1*], Leisheng Zhang[2,3,4,5*], Jianhua Gao[6*], Ti'er Wang[7*], Min Liu[7], Xiaoming Feng[7], Xianghong Xu[2], Shixun Ma[2], Hui Cai[2], Tiankang Guo[2], Weibin Huang[8], Xiaoyan Tu[8], Shuling Wang[8], Hongju Yang[9], Yihu Fang[6], Feifei Li[10], Cunrong Chen[8]

[1]Reproductive Medicine Center, The First Affiliated Hospital of Hainan Medical University, Key Laboratory of Reproductive Health Diseases Research and Translation (Hainan Medical University), Ministry of Education, Haikou 570102, Hainan, China; [2]Key Laboratory of Molecular Diagnostics and Precision Medicine for Surgical Oncology in Gansu Province & NHC Key Laboratory of Diagnosis and Therapy of Gastrointestinal Tumor, Gansu Provincial Hospital, Lanzhou 730000, Gansu, China; [3]Key Laboratory of Radiation Technology and Biophysics, Hefei Institute of Physical Science, Chinese Academy of Sciences, Hefei 230031, Anhui, China; [4]Jiangxi Research Center of Stem Cell Engineering, Jiangxi Health-Biotech Stem Cell Technology Co., Ltd., Shangrao 334000, Jiangxi, China; [5]Department of General Practice, Affiliated Hospital of Xiangnan University, Chenzhou 423000, Hunan, China; [6]Institute of Stem Cell, Jiangxi Medical College, Shangrao 334000, Jiangxi, China; [7]State Key Laboratory of Experimental Hematology, National Clinical Research Center for Blood Disease, Haihe Laboratory of Cell Ecosystem, Institute of Hematology & Blood Diseases Hospital, Chinese Academy of Medical Sciences & Peking Union Medical College, Tianjin 300020, China; [8]Department of Critical Care Medicine, Fujian Medical University Union Hospital, Fuzhou 350001, Fujian, China; [9]Division of Gastroenterology, The First Affiliated Hospital of Kunming Medical University, Kunming 650031, Yunnan, China; [10]Department of Pathophysiology, School of Basic Medical Sciences, Anhui Medical University, Hefei 230032, Anhui, China. [*]Equal contributors.

Received December 21, 2022; Accepted May 4, 2023; Epub May 15, 2023; Published May 30, 2023

Abstract: Longitudinal studies have highlighted allogeneic natural killer (NK) cell-based cytotherapy for cancer immunosurveillance and immunotherapy, yet the deficiency of systematic and detailed comparison of NK cells from candidate sources including umbilical cord blood (UC) and bone marrow (BM) largely hinders the large-scale application. Herein, we isolated resident NK cells (rUC-NK, rBM-NK) from mononuclear cells (MNC), and analyzed the corresponding expanded NK cell counterparts (eUC-NK, eBM-NK). Then, the eUC-NK and eBM-NK were turned to multifaceted bioinformatics from the aspects of gene expression profiling and genetic variations. The percentages of total or activated NK cells in rBM-NK group were approximate 2-fold higher over those in the rUC-NK group, respectively. Instead, the proportion of total NK cells in eUC-NK was higher than that in the eBM-NK group, and in particular, the $CD25^+$ memory-like NK cell subset. Furthermore, eUC-NK and eBM-NK manifested multidimensional similarities and diversities in gene expression pattern and genetic spectrum, whereas both eUC-NK and eBM-NK exhibited effective tumor killing capacity. Collectively, we dissected the cellular and transcriptomic signatures of NK cells generated from UC-MNC and BM-MNC, which supplied new literature for further exploring the characteristics of the indicated NK cells and would benefit the clinical application for cancer immunotherapy in future.

Keywords: Natural killer cells, umbilical cord blood, biological signatures, transcriptomic characteristics, cancer immunotherapy

Introduction

As one of the life-threatening diseases with high morbidity and mortality, cancers have emerged as a heavy burden for individual patients and economic society worldwide [1, 2]. For example, cancers were recognized as the second most common causes of death among kids in America, and over 10,000 children and 5,000 adolescents were diagnosed with cancers in 2021 [1]. For decades, we and other investigators in the field have been devoted to

figure out the pathogenesis of cancers from the view of genetic variations and environmental stimulus such as heterogeneity, uncontrolled cell division, cancer stem cells (CSCs), proto-oncogenes and anti-oncogenes, Ionizing radiation, dangerous carcinogens, and even the coronavirus disease 2019 (COVID-19) pandemic [3-6].

To date, a variety of treatment regiments have arisen for oncotherapy, including surgery (e.g., robotic surgery, laparoscopic rectal surgery), chemotherapy, oncolytic virotherapy, radiotherapy, hormone therapy, photothermal therapy, peptide-based neoantigen vaccine, RNA vaccine, nanotheranostics and immunotherapy [7-11]. Despite the considerable advancements in cancer administration, more effective implementation remedies are still urgently needed for the improvement of the incidence and survival rates and the concomitant optimization of cancer diagnosis and treatment [12, 13]. For instance, the progress in medical practice has strengthened for lung cancer but stagnated for prostate and breast cancers instead [5]. Of note, state-of-the-art renewal has highlighted the feasibility of cancer immunotherapy as a revolutionizing and promising route for targeted cancer control interventions and the resultant reductions in cancer mortality [6, 8, 14].

Natural killer (NK) cells are heterogeneous populations and play a vital role in both innate and adoptive immune responses dispense with preliminary antigen presentation attributes to the non-MHC-restricted recognition [7, 12, 15]. For decades, NK cells have been generated from perinatal blood (e.g., umbilical cord blood, placental blood) and adult blood (e.g., bone marrow, peripheral blood), NK cell lines (e.g., NK-92, YT), and even stem cells (e.g., hematopoietic stem cells, pluripotent stem cells) [7, 16-21]. Bone marrow-derived NK cells are lymphocytes resided in the hematopoietic microenvironment, which have been recognized as crucial constituents for host defense against diverse infections and tumors [22]. Currently, due to the deficiency of peripheral blood, umbilical cord blood has been regarded as alternative source for high-efficient NK cell generation and cancer immunotherapy [7, 23, 24]. However, the systematic and detailed information of the similarities and variations between the tissue resident or *ex vivo* expanded BM-NK cells and UC-NK cells is still largely obscure, which will largely hinder the further development of allogeneic NK cell-based novel regimens.

For the purpose, in this study we utilized our well-established "3IL"-based strategy for *ex vivo* NK cell induction from umbilical cord blood- and bone marrow-derived mononuclear cells (MNCs). With the aid of multifaceted cellular evaluation and high-throughput sequencing, we verified the similarities and distinctions of the aforementioned NK cells in biological properties (e.g., immunophenotype, cellular vitality, activation and cytotoxicity) and transcriptomic landscapes (e.g., gene expression profiling, gene ontology, signaling pathway, genetic variations). Taken together, our data provide new references for decoding the biological and transcriptomic signatures of UC-NK cells with BM-NK cells, which will benefit the further investigations upon NK cell-based cancer immunotherapy.

Materials and methods

Enrichment of mononuclear cells (MNCs)

Human bone marrow tissue and umbilical cord blood were obtained from healthy donors with the approval of the Ethics Committee of Shangrao ETD-H&B Hospital (KLL-2020-04) and Gansu Provincial Hospital (2023-120) according to the guidelines of Helsinki. In general, BM-MNCs and UC-MNCs were isolated by utilizing the standard Ficoll (Sigma-Aldrich, USA)-based density gradient centrifugation method as we recently described [19, 25].

In vitro NK cell induction from MNCs

In vitro amplification and activation of NK cells were conducted as we recently reported by utilizing our well-established "3IL"-based strategy. In details, 2 × 10^6/ml BM-MNCs or UC-MNCs were seeded in NK MACS Medium (Miltenyi Biotech, Germany) supplemented with cytokine cocktail addition (rhIL-2, 1000 U/mL; rhIL-15, 10 ng/ml; rhIL-18, 50 ng/ml) [19]. The medium was half changed every two days until day 14. Trypan Blue staining and flow cytometry (FCM) assay were used for cell counting and quantification, respectively. The list of the cytokines was available in Supplementary Table 1.

Flow cytometry (FCM) assay

FCM assay was employed for the proportion analyses of total NK cells ($CD3^-CD56^+$), specific NK cell subsets ($CD16^+$, $CD25^+$, $NKp44^+$, $NKp46^+$, $NKG2D^+$) and relative populations ($CD4^+$, $CD8^+$, Annexin V^+, 7-AAD^+, $CD107a^+$) as we described before [20, 21]. In details, the MNCs (UC-MNCs, BM-MNCs), resident NK cells (rUC-MNCs, rBM-MNCs), and expanded NK cells (eUC-MNCs, eBM-MNCs) were incubated with the indicated fluorescence conjugated antibodies in dark for 30 min, and washed with 1 × PBS for further detection. Then, the aforementioned cells were turned to FACS Canto II (BD Biosci, USA) and FlowJo 10.0 software (Tree Star, USA) for analysis, respectively. The list of the antibodies was available in Supplementary Table 2.

Cellular vitality assay

The cellular vitality of the indicated NK cells was accomplished with cell cycle assay and apoptosis assay as we recently reported [19, 21]. For cell cycle assay, NK cells were pretreated with 70% (v/v) cooled ethanol and fixed at 4°C. After washing with 1 × PBS, the cells were turned to Propidium iodide (PI) staining and BD LSR II (BD Biosci, USA) for analysis. For cell apoptosis assay, 1×10^6 cells were washes with precooled 1 × PBS and incubated with the Annexin V Apoptosis Detection Kit including Annexin V-FITC and 7-AAD solution (Sigma-Aldrich, USA). Finally, the cells were turned to FACS Canto II (BD Biosci, USA) for apoptotic cell analysis.

RNA-sequencing (RNA-SEQ) and bioinformatics analysis

For total mRNA preparation, eUC-NK and eBM-NK at day 14 were lysed with TRIZol reagent (ThermoFisher, USA) according to the manufacturer's instructions [21, 26]. The mRNAs were turned to BGI Genomics (Shenzhen, China) for sequencing. The bioinformatics analysis such as Principal Component Analysis (PCA), HeatMap, Volcano Plot, hierarchical cluster analysis, Gene Set Enrichment Analysis (GSEA, https://www.gsea-msigdb.org/gsea/index.jsp), Gene Ontology (GO, http://geneontology.org/), Kyoto Encyclopedia of Genes and Genomes (KEGG, https://www.kegg.jp/) were conducted as we recently described [27, 28]. The list of DEGs between eBM-NKs and eUC-NKs was available in Supplementary Table 3.

Cytotoxicity assessment of NK cells

The cytotoxicity of the indicated eUC-NK cells and eBM-NK cells was performed as we previously reported [19, 20]. Generally, tumor cell lines (K562, Nalm6, U937) were harvested and labelled with CellTrace Violet (Invitrogen, USA) as we described with several modifications [19, 29]. Then, the eUC-NK cells or eBM-NK cells were cocultured with the aforementioned tumor cells at an effector-to-target ratios (E:T= 1:1) for 8 hrs. After that, the cells were labeled with the indicated antibodies (e.g., anti-CD3, ant-CD56, ant-CD16, anti-CD107a, 7-AAD) and Precision Count Beads (BioLegend, USA). Finally, the incubated cells were washed with 1 × PBS and tested by FACS Canto II (BD Biosci, USA). NK cell Cytotoxicity = $(1 - N_2/N_1) \times 100\%$. N_1 represents the total number of living tumor cells in control group, N_2 represents the total number of living tumor cells in the experimental group [19, 21].

Statistical analyses

All statistical analyses were accomplished with the Graph Pad Prism 6.0 (San Diego, USA) software as we previously described [30, 31]. The student's unpaired T test was conducted to analyze the data between two unpaired groups, whereas the one-way ANOVA test was utilized to analyze the data among multiple unpaired groups. Data were shown as mean ± SEM (N=3 independent experiments), when *P* value <0.05 was recognized as statistically significant. NS, not significant; *, P<0.05; **, P< 0.01; ***, P<0.001; ****, P<0.0001.

Results

Resident NK cells in bone marrow revealed higher proportion and activity over those in umbilical cord blood

To assess the potent similarities and distinctions of NK cells generated from bone marrow and umbilical cord blood, we initially enriched MNCs and explored the corresponding resident NK cells (rNK). According to the FCM diagrams, the proportions of $CD3^-CD56^+$ total NK cells and $CD3^-CD56^+CD16^+$ activated NK cells in the rBM group were approximate 2-fold high-

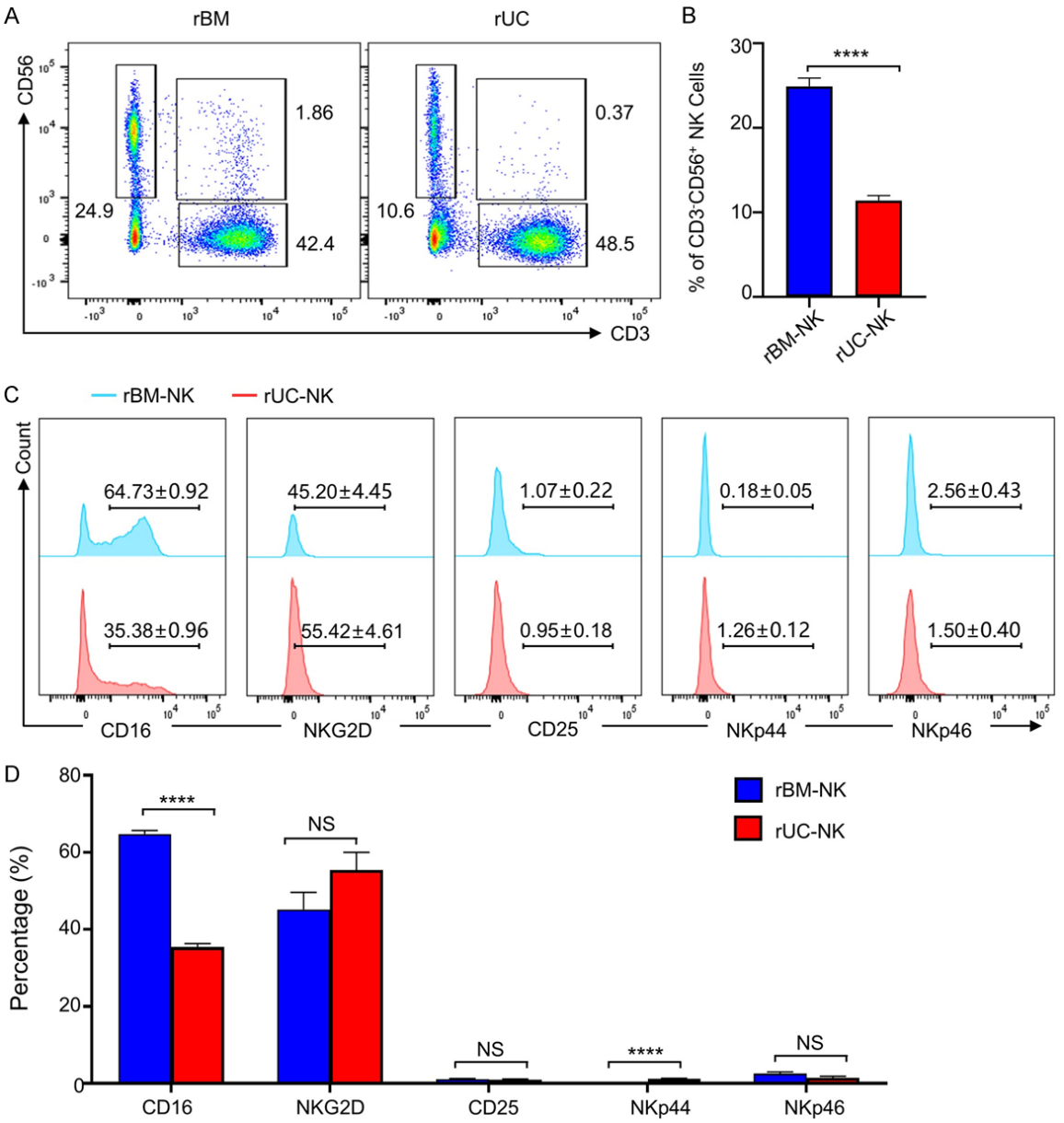

Figure 1. The comparison of resident NK cells in MNCs enriched from bone marrow and umbilical cord blood. (A, B) Representative flow cytometry (FCM) diagrams (A) and statistical analysis (B) of resident bone marrow-derived mononuclear cells (rBM) and umbilical cord blood-derived mononuclear cells (rUC). (C, D) Representative FCM diagrams (C) and statistical analysis of the NK cell (D) subpopulations of rBM-NK and rUC-NK. All data were shown as mean ± SEM (N=3). NS, not significant; ****, P<0.0001.

er than those in the rUC, respectively (**Figure 1A-D**). Furthermore, except for the $CD3^-CD56^+NKp44^+$ subset, minimal differences were observed in the percentages of other activated NK cell subsets such as the $NKG2D^+$, $NKp46^+$ and $CD25^+$ counterparts (**Figure 1C**, **1D**). Taken together, BM-MNCs rather than UC-MNCs revealed higher percentages of total and activated rNK cells.

Expanded NK cells from UCB manifested superiority in amplification over those generated from BM but with comparable cellular vitality

Having dissected the rNK in BM-MNCs and UC-MNCs, we next turn to explore the biological signatures of the corresponding expanded NK cells (eBM-NK, eUC-NK) by utilizing our well-established "3IL"-based strategy [19, 21]. As

shown by the phase contrast images, the seeded cells (day 0) in both BM-NK and UC-NK groups revealed unicellular morphology, and more typical NK cell clusters were arisen during the *ex vivo* induction (**Figure 2A**). Compared to the BM-NK group, approximate 2-fold change of eNK cells was observed in the UC-NK group at day 14 (**Figure 2B**).

Simultaneously, we took advantage of FCM analyses to evaluate the cellular vitality of eNK at day 14. As shown by the FCM diagrams and statistical analysis, no significant differences were observed in the percentage of apoptotic NK cells (**Figure 2C**, **2D**). Furthermore, with the aid of cell cycle assay, we noticed that the proportion of G0/G1 subset rather than the G2/M subset in the eBM-NK group was moderately higher over that in the eUC-NK group (**Figure 2E**, **2F**). Collectively, our data indicated the preferable *ex vivo* amplification property of eUC-NK over eBM-NK, together with the minimal differences in cellular vitality.

Expanded NK cells and resident NK cells exhibited multifaceted diversity in subpopulations

To further explore the cellular phenotypes of eUC-NK and eBM-NK, we conducted FCM assay and found that the percentages of both $CD3^-CD56^+$ total NK cells and $CD3^-CD56^+CD25^+$ memory-like NK cells were much higher in the eUC group after the 14-day's *ex vivo* expansion and activation, whereas the proportion of $CD3^-CD56^+NKp44^+$ activated NK cell subset was lower compared to the eBM group instead (**Figure 3A-D**). Distinguish from those in the rNK, we noticed there were minimal differences in the percentage of $CD3^-CD56^+CD16^+$ total activated NK cell between the eBM-NK and eUC-NK group (**Figure 3D**). Similarly, the proportions of $CD3^-CD56^+$ total NK cells and activated NK cell subsets in eNK (eBM-NK, eUC-NK) at day 14 were consistently elevated and higher than the corresponding rNK (rBM-NK, rUC-NK) at day 0 except for the $CD3^-CD56^+CD16^+$ total activated NK cells in the rBM-NK and eBM-NK groups, respectively (**Figure 3E**, **3F**). Overall, these findings indicated the further maturation of rNK towards eNK as well as high-efficient *ex vivo* NK cell generation after the "3IL"-based stimulation, and in particular, the eUC-NK with more robust amplification and activation properties.

The gene expression profiling of expanded BM-NK cells and UC-NK cells manifested multidimensional similarity and diversity

Having illuminated the biological properties of the eNK, we were next curious about the multifaceted characteristics at molecular levels. For the purpose, we took advantage of RNA-SEQ for transcriptomic analysis of eBM-NK (eBM-NK-1, eBM-NK-2, eBM-NK-3) and eUC-NK (eUC-NK-1, eUC-NK-2, eUC-NK-3). Initially, as shown by the stacked bar chart and Violin Plot diagrams, we noticed the similarities between eBM-NK and eUC-NK in overall gene expression pattern (**Figure 4A**, **4B**). In details, the distribution of the significantly upregulated and downregulated differently expressed genes (DEGs) genes as well as the non-DEGs between the indicated eNK were intuitively shown by the Volcano Plot (**Figure 4C**).

Simultaneously, with the aid of principal component analysis (PCA) and correlation analysis, the genetic relationship of individual eBM-NK and eUC-NK were visually presented (**Figure 4D**, **4E**). Furthermore, by conducting the hierarchical cluster analysis based on TPM (transcripts per kilobase of exon model per million mapped reads) values of DEGs, we found eBM-NK (eBM-NK-1, eBM-NK-2, eBM-NK-3) and eUC-NK (eUC-NK-1, eUC-NK-2, eUC-NK-3) revealed preferable relatedness within groups rather than between groups, respectively (**Figure 4F**). Subsequently, with the aid of gene ontology biological process (GOBP) assay of DEGs, we noticed cancer immunotherapy-associated biological processes such as immune response, negative regulation of cell proliferation, ERK1/2 cascade, and chemotaxis were specifically enriched (**Figure 4G**). Similarly, according to the GOBP assay of the differentially expressed transcripts, we observed the enrichment of transcription-associated processes including positive or negative regulation of transcription, chromatin organization, and regulation of immune response (**Figure 4H**). Collectively, eBM-NK and eUC-NK manifested multifaceted similarities and diversities in gene expression profiling, which further indicated the consistency and variations with the biological properties.

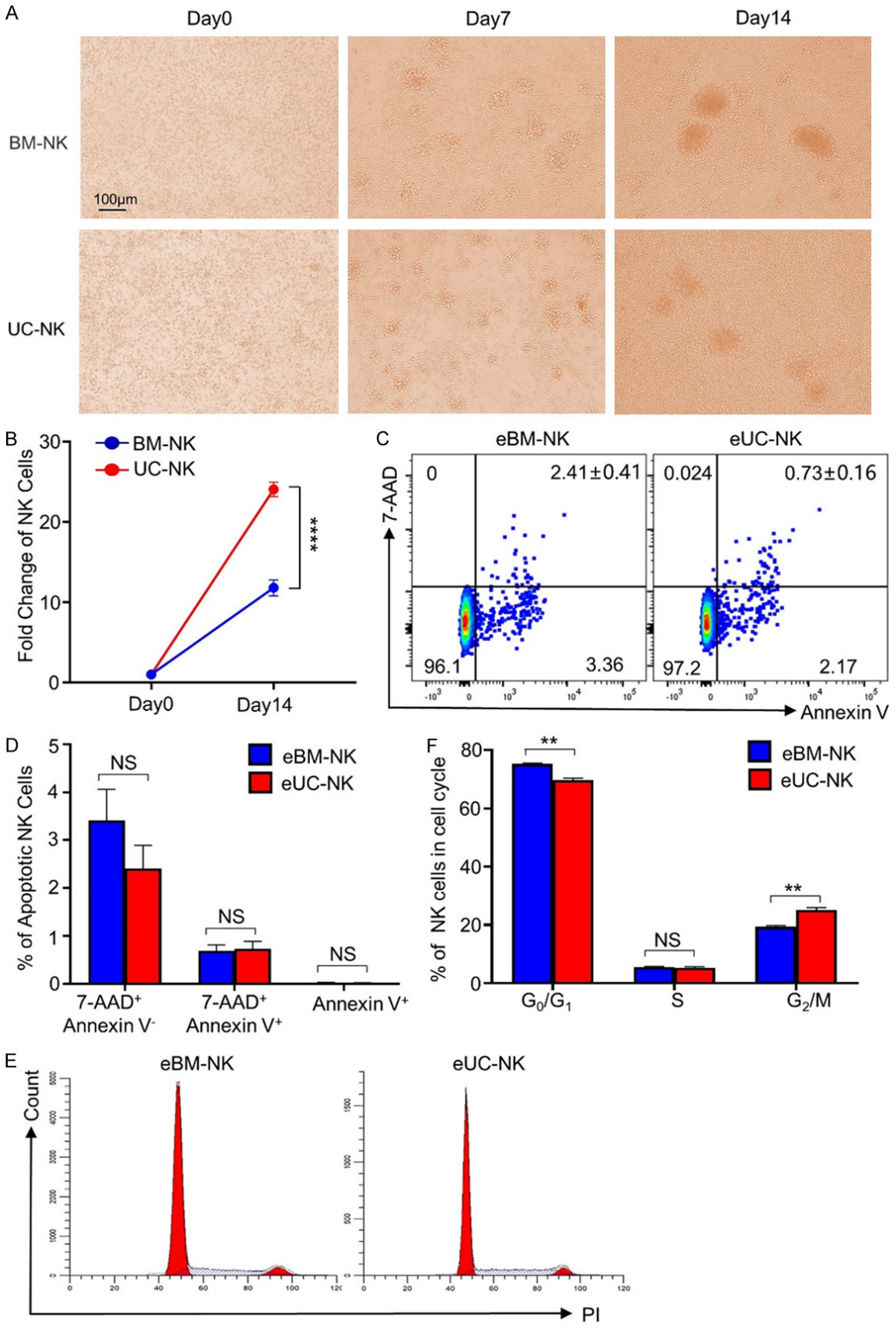
A
Day0
Day7
Day14
BM-NK
UC-NK
100μm
B
BM-NK
UC-NK
Fold Change of NK Cells
****
Day0
Day14
C
eBM-NK
eUC-NK
7-AAD
0
2.41±0.41
96.1
3.36
0.024
0.73±0.16
97.2
2.17
Annexin V
D
eBM-NK
eUC-NK
% of Apoptotic NK Cells
NS
NS
NS
7-AAD+ Annexin V-
7-AAD+ Annexin V+
Annexin V+
F
eBM-NK
eUC-NK
% of NK cells in cell cycle
**
NS
**
G0/G1
S
G2/M
E
eBM-NK
eUC-NK
Count
PI

Figure 2. The comparison of the expanded NK cells in content and cellular vitality. (A) Representative phase contract images of MNC-derived NK cells with our well-established "3IL"-based strategey. Scale bar =100 μm. (B) Fold change of NK cells from the resident NK cells (rNK) at day 0 to the corresponding expanded NK cells (eNK) at day 14. The fold changes were normalized to rNK at day 0. (C, D) Representative FCM diagrams (C) and statistical analysis (D) of apoptotic NK cells in eBM-NK and eUC-NK at day 14. (E, F) The representative distribution (E) and statistical analysis (F) of eBM-NK and eUC-NK in the indicated substages of cell cycle. All data were shown as mean ± SEM (N=3). NS, not significant; **, P<0.01; ****, P<0.0001.

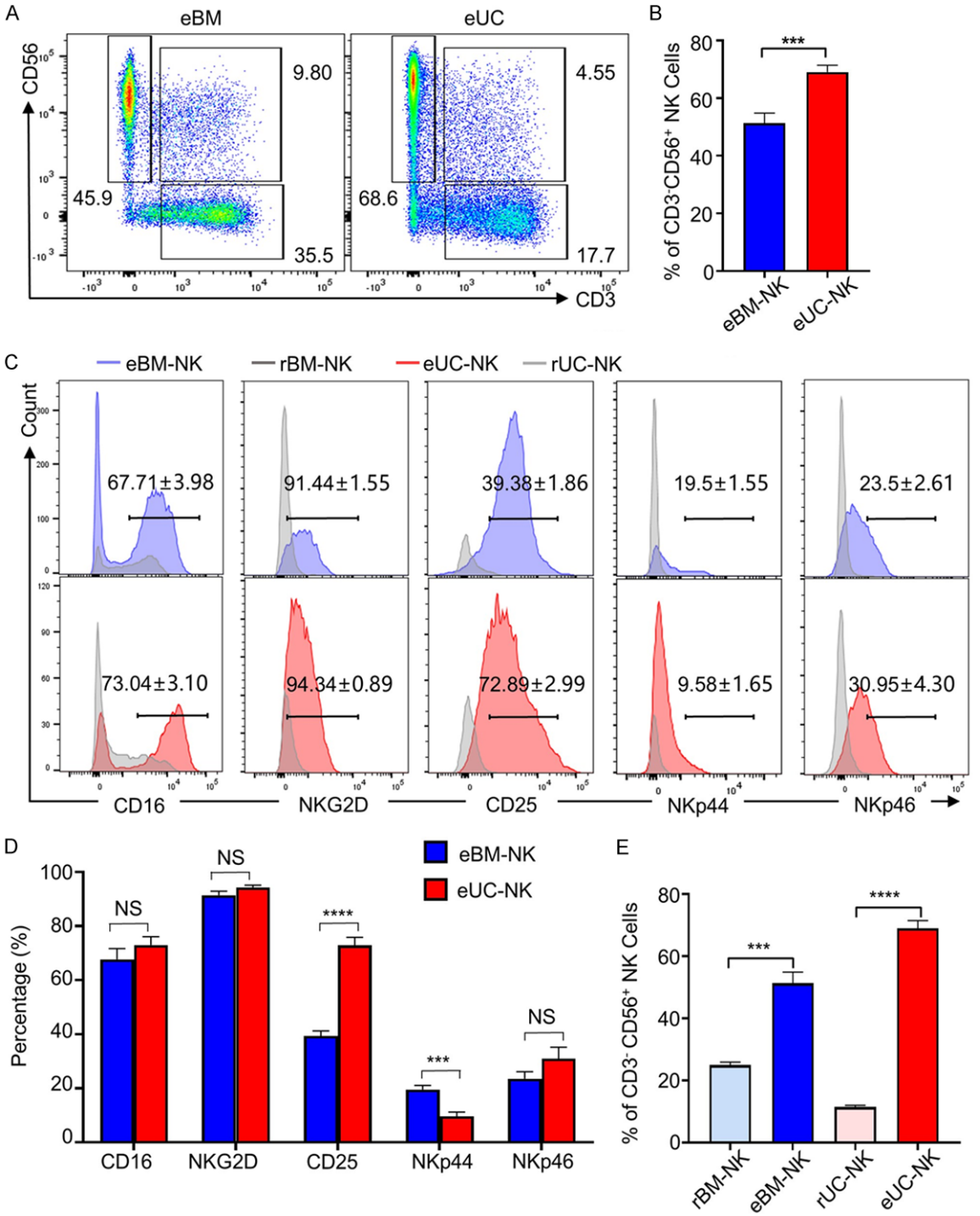

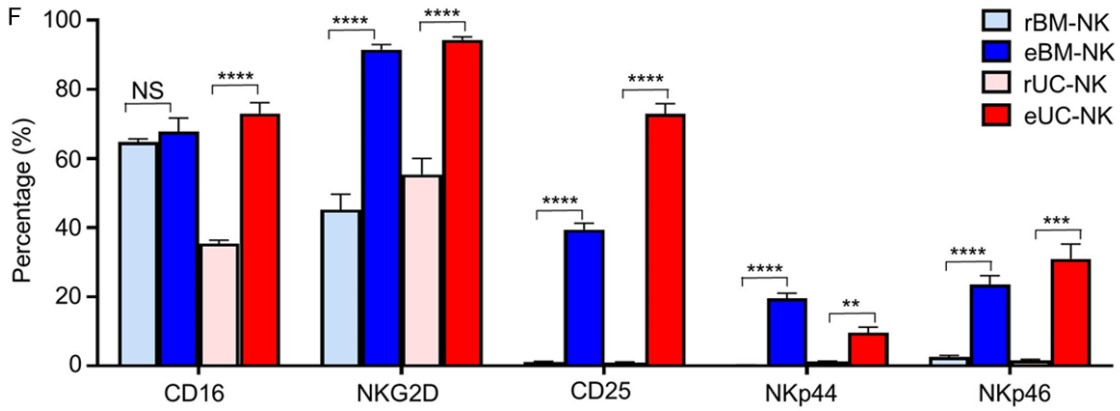

Figure 3. The comparison of resident NK cells and expanded NK cells. (A, B) Representative FCM diagrams (A) and statistical analysis (B) of eBM and eUC at day 14. (C, D) Representative FCM diagrams (C) and statistical analysis (D) of the NK cell subpopulations in rNK (rBM-NK, rUC-NK) at day 0 and the corresponding eNK (eBM-NK, eUC-NK) at day 14. (E, F) Statistical analysis of total NK cells (E) and NK cell subpopulations (F) among the indicated rNK (rBM-NK, rUC-NK) and eNK (eBM-NK, eUC-NK). All data were shown as mean ± SEM (N=3). NS, not significant; ***, P<0.001; ****, P<0.0001.

The landscapes of signaling pathway and variation spectrum of expanded BM-NK cells and UC-NK cells

To further estimate the genetic characteristics of the indicated eNK, we turned to kyoto encyclopedia of genes and genomes (KEGG) analysis, and found that the DEGs were mainly involved in cytokine-cytokine receptor interaction-, antigen processing and presentation-, NK cell mediated cytotoxicity-, TGF-β signaling pathway-, NF-Kappa B signaling pathway-, and chemokine signaling pathway-related processes (**Figure 5A**). The KEGG network assay of the aforementioned DEGs further intuitively revealed the relevance of the central signaling pathways (**Figure 5B**). Therewith, by conducting gene set enrichment analysis (GSEA), we observed the specific enrichment of the significantly different gene sets between eBM-NK and eUC-NK such as PPAR signaling pathway, TLR1/2 ligand vs NOD2 monocyte, fatty acid metabolism and glycolysis, whereas minimal differences were shown in KARS signaling pathway and complement and coagulation cascades (**Figure 5C**, **5D**). Furthermore, the protein-protein interaction (PPI) network and KDA diagram consistently reflected the profile of the spatial relationship of the representative core DEGs, including CCL2, JUN, CD40LG, IFNG, TNF, and FOXP3 (**Figure 5E**, **5F**).

For the purpose of further illuminating the potential similarities and differences in genetic modifications accompanied with the DEGs between the indicated eNK, we meticulously compared the overview of variable shear event (VSE), and verified the similarity in as_a3ss, as_a5ss, as_mxe, as_ri and as_se distribution (**Figure 5G**). Furthermore, among the differentially VSE (DVSE), the as_se subset were the principal variations in genetic modification (**Figure 5H**). Additionally, as shown by the Circos diagrams, the loci regional distribution of the indicated somatic variations such as gene fusion events, SNPs, INDELs and FPKM values could be intuitively observed in the chromosomes of eBM-NK and eUC-NKs (**Figure 5I**). Collectively, these data indicated the multidimensional conservations and alterations in the spectrum of genetic modifications between eBM-NK and eUC-NKs.

Expanded BM-NK cells and UC-NK cells showed effective lethality towards multiple tumor cells in vitro

Due to the boundedness of rNK in quantity and immaturity, we turned to the eNK for *ex vivo* cytotoxic assessment. Therefore, we took advantage of the NK cell and tumor cell line co-culture model at the effector-target ratio (E:T=1:1), and verified that eBM-NKs revealed a higher percentage of $CD107^+$ subset than that in eUC-NK against K562 and U937 cells, whereas no significant differences were observed against Nalm6 cells (**Figure 6A**, **6B**). Meanwhile, the cytotoxicity of eBM-NKs against the target

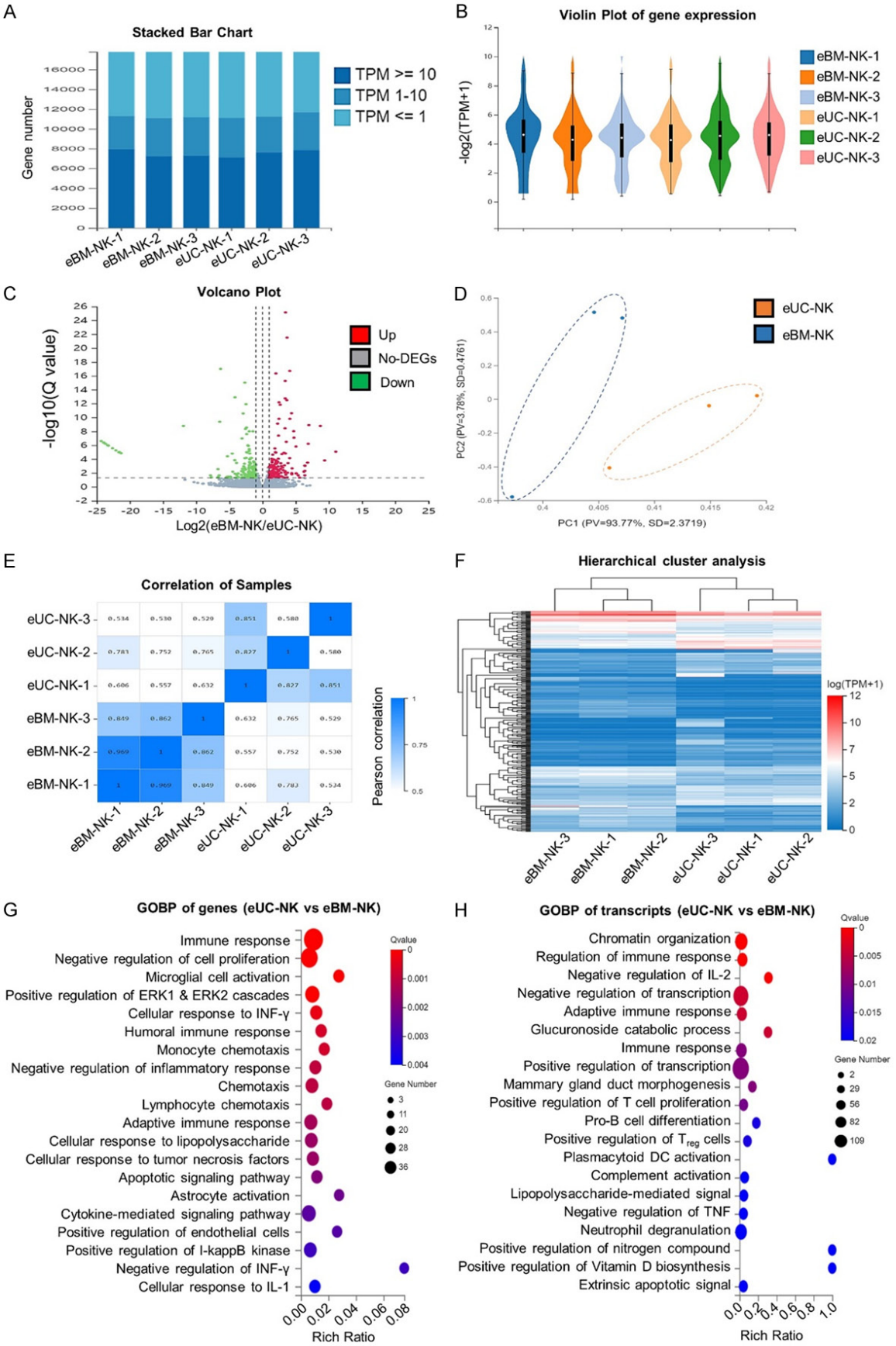
A
Stacked Bar Chart
Gene number
TPM >= 10
TPM 1-10
TPM <= 1
eBM-NK-1
eBM-NK-2
eBM-NK-3
eUC-NK-1
eUC-NK-2
eUC-NK-3
B
Violin Plot of gene expression
-log2(TPM+1)
C
Volcano Plot
-log10(Q value)
Log2(eBM-NK/eUC-NK)
Up
No-DEGs
Down
D
eUC-NK
eBM-NK
PC2 (PV=3.78%, SD=0.4761)
PC1 (PV=93.77%, SD=2.3719)
E
Correlation of Samples
Pearson correlation
F
Hierarchical cluster analysis
log(TPM+1)
G
GOBP of genes (eUC-NK vs eBM-NK)
Immune response
Negative regulation of cell proliferation
Microglial cell activation
Positive regulation of ERK1 & ERK2 cascades
Cellular response to INF-γ
Humoral immune response
Monocyte chemotaxis
Negative regulation of inflammatory response
Chemotaxis
Lymphocyte chemotaxis
Adaptive immune response
Cellular response to lipopolysaccharide
Cellular response to tumor necrosis factors
Apoptotic signaling pathway
Astrocyte activation
Cytokine-mediated signaling pathway
Positive regulation of endothelial cells
Positive regulation of I-kappB kinase
Negative regulation of INF-γ
Cellular response to IL-1
Qvalue
Gene Number
Rich Ratio
H
GOBP of transcripts (eUC-NK vs eBM-NK)
Chromatin organization
Regulation of immune response
Negative regulation of IL-2
Negative regulation of transcription
Adaptive immune response
Glucuronoside catabolic process
Immune response
Positive regulation of transcription
Mammary gland duct morphogenesis
Positive regulation of T cell proliferation
Pro-B cell differentiation
Positive regulation of Treg cells
Plasmacytoid DC activation
Complement activation
Lipopolysaccharide-mediated signal
Negative regulation of TNF
Neutrophil degranulation
Positive regulation of nitrogen compound
Positive regulation of Vitamin D biosynthesis
Extrinsic apoptotic signal
Qvalue
Gene Number
Rich Ratio

Figure 4. Comparison of gene expression profiling of eBM-NK and eUC-NK. (A) The stacked bar chart of gene numbers with the indicated expression levels based on TPM values in eBM-NK (eBM-NK-1, eBM-NK-2, eBM-NK-3) and eUC-NK (eUC-NK-1, eUC-NK-2, eUC-NK-3). (B, C) The violin plot (B) and Volcano plot (C) of gene expression pattern in the aforementioned eBM-NK and eUC-NK. (D) The PCA analysis of the indicated eBM-NK and eUC-NK based on FPKM values. (E) The correlation of affinity among the indicated eBM-NK and eUC-NK. (F) HeatMap diagram of the differentially expressed genes (DEGs) in eBM-NK and eUC-NK. (G, H) The gene ontology biological process (GOBP) assay based on the differentially expressed genes (G) and transcripts (H) between eBM-NK and eUC-NK.

Nalm6 cells rather than the K562 and U937 tumor cells was equal to that of eUC-NKs, which was confirmed by BV421-based fluorescence according to the statistical analyses (**Figure 6C**, **6D**). Taken together, our data suggested that the eBM-NK revealed moderate advantage over eUC-NK in *ex vivo* cytotoxicity.

Discussion

Cancers, including the metastatic solid tumors and hematologic malignancies, have caused thousands on thousands of deaths worldwide due to the high morbidity and mortality. In spite of the encouraging breakthroughs in cancer amelioration and treatment, yet the favorable and persistent prognosis of cancer patients are still challenging and urgently to be improved. Of note, state-of-the-art literatures have highlighted the rosy prospect of adoptive NK cell-based cytotherapy for cancer immunotherapy, yet the large-scale application in clinical practices are largely restricted to the deficiency of systematic and detailed dissection of the signatures at cellular and molecular levels. Herein, we took advantage of the "3IL"-based procedure for *ex vivo* amplification and activation of rNK into eNK, and verified the multidimensional biological properties and transcriptomic characteristics of NK cells derived from bone marrow and umbilical cord blood, together with the cytotoxicity assessment against tumor cell lines, which would collectively benefit the further exploration of NK cell-based remedies for cancer administration.

For decades, surgeries (e.g., robotic surgery) in combination with chemoradiotherapy (e.g., radiotherapy, chemotherapy) and drug therapy have been considered as classical therapeutic modalities for localized cancers without diffusion and metastasis [10, 32]. In recent years, novel strategies in the field of cancer immunotherapy including autogenous and allogeneic immune cells (e.g., TILs, CILs, NK cells, CAR-T cells, CAR-NK cells), lymphocyte-promoting cytokines (e.g., GM-CSF, IFN-γ), checkpoint inhibitors (e.g., PD-L1, CTLA4), cancer vaccines (e.g., mRNAs), and monoclonal antibodies (mAb) has been continuously developed to fulfil cancer management [33-36]. Of note, chimeric antigen receptor-transduced T lymphocytes (CAR-Ts) have been proved by preclinical and clinical investigations with remarkable efficacy for various hematological malignancies such as B-cell non-Hodgkin's lymphoma (NHL) and relapsed B acute lymphoblastic leukemia (r/rB-ALL) [37-41]. Similarly, T cell receptor-engineered T cells (TCR-Ts) are recognized as splendid alternatives to eliminate a relatively broad range of cancers by redirecting the recognition capability of cancer-associated surface antigens [42]. Distinguish from the aforementioned remedies, adoptive NK cells or CAR-NK cells hold advantaged superiority in cancer immunotherapy via simultaneously modulating the innate and adaptive immunity dispense with antigen presentation and sensitization. Moreover, the NK cell-based immunotherapy is not inclined to cause severe adverse reactions including graft-versus-host disease (GvHD), immune cell-associated neurotoxicity syndrome (ICANS), cytokine release syndrome (CRS) [12, 43, 44]. Therefore, NK cells and CAR-NKs are currently considered as "off-the-shelf" products and a promising virgin ground of cancer immunotherapy and immunosurveillance innovation.

For decades, we and other investigators in the field have been devoted to fulfilling the goal of relapse and recurrent cancer administration by utilizing the NK cell-based immunotherapy for boosting the immune system to strengthen anti-cancer responses and eventually obliterate the metastatic malignancies [7, 45, 46]. For instance, we have conducted continuous optimization of *ex vivo* procedures for large-scale preparation of NK cells with preferable cellular vitality and elevated cytotoxicity against a series of tumor cells, including initiating cell source selection (e.g., NK-92, KHYG-1, PBMCs, UC-MNCs, BM-MNCs, placental tissue, $CD3^-$

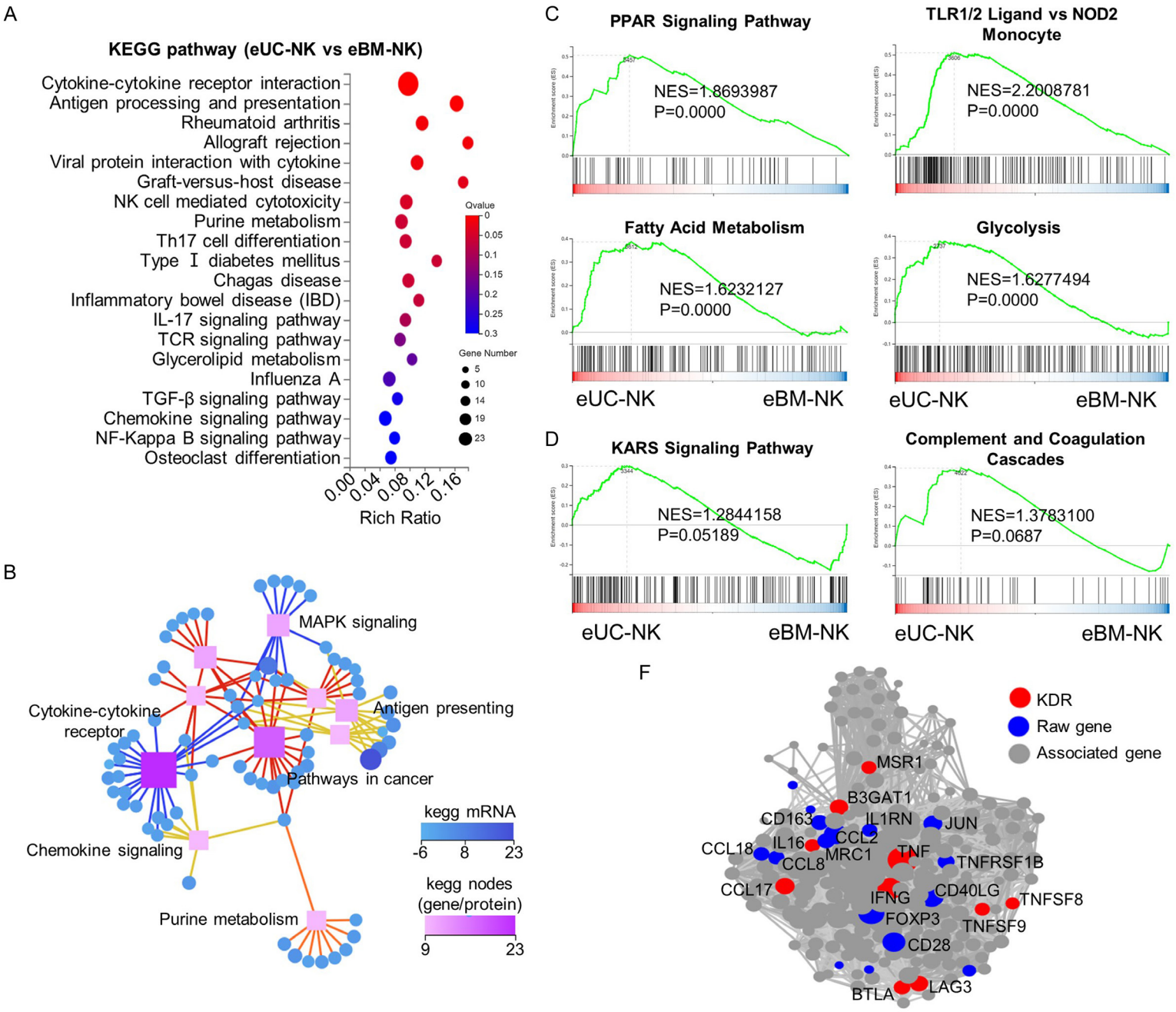
A
KEGG pathway (eUC-NK vs eBM-NK)
Cytokine-cytokine receptor interaction
Antigen processing and presentation
Rheumatoid arthritis
Allograft rejection
Viral protein interaction with cytokine
Graft-versus-host disease
NK cell mediated cytotoxicity
Purine metabolism
Th17 cell differentiation
Type I diabetes mellitus
Chagas disease
Inflammatory bowel disease (IBD)
IL-17 signaling pathway
TCR signaling pathway
Glycerolipid metabolism
Influenza A
TGF-β signaling pathway
Chemokine signaling pathway
NF-Kappa B signaling pathway
Osteoclast differentiation
0.00 0.04 0.08 0.12 0.16
Rich Ratio
Qvalue
0 0.05 0.1 0.15 0.2 0.25 0.3
Gene Number
5 10 14 19 23
B
MAPK signaling
Cytokine-cytokine receptor
Antigen presenting
Pathways in cancer
Chemokine signaling
Purine metabolism
kegg mRNA
-6 8 23
kegg nodes (gene/protein)
9 23
C
PPAR Signaling Pathway
NES=1.8693987
P=0.0000
TLR1/2 Ligand vs NOD2 Monocyte
NES=2.2008781
P=0.0000
Fatty Acid Metabolism
NES=1.6232127
P=0.0000
Glycolysis
NES=1.6277494
P=0.0000
eUC-NK
eBM-NK
D
KARS Signaling Pathway
NES=1.2844158
P=0.05189
Complement and Coagulation Cascades
NES=1.3783100
P=0.0687
eUC-NK
eBM-NK
F
KDR
Raw gene
Associated gene
MSR1
B3GAT1
CD163
IL1RN
JUN
CCL2
IL16
CCL18
MRC1
TNF
CCL8
TNFRSF1B
CCL17
IFNG
CD40LG
TNFSF8
FOXP3
TNFSF9
CD28
BTLA
LAG3

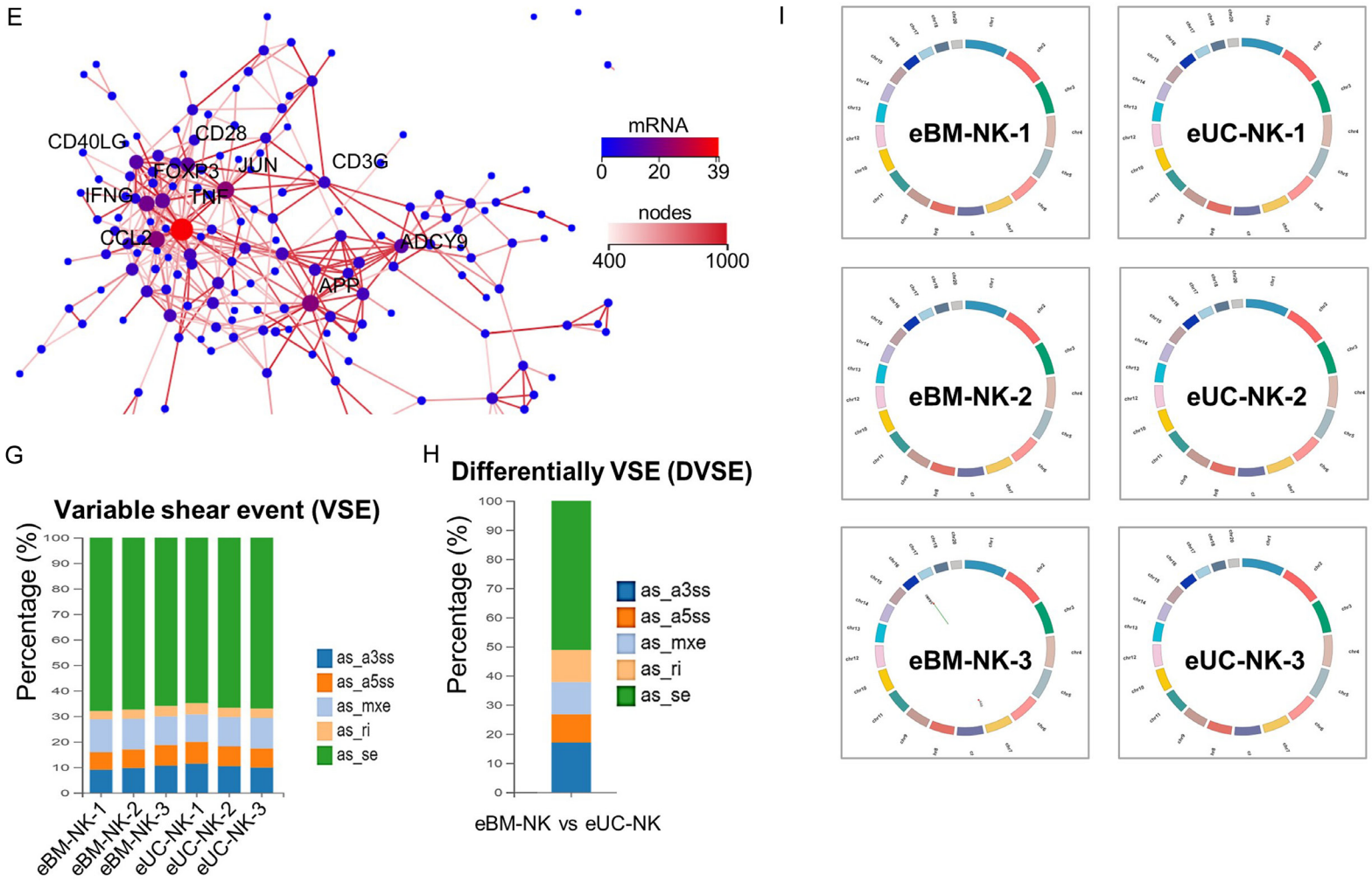

Figure 5. Signaling pathway analysis and variation spectrums between eBM-NK and eUC-NK. (A, B) KEGG analysis (A) and pathway correlation assay (B) of hAMSCs in eBM-NK and eUC-NK based on DEGs. (C, D) GSEA diagrams of significantly different gene sets (C) and non-different gene sets (D) between eBM-NK and eUC-NK. (E) PPI analysis of the DEGs (log_2FC >1.0) between eBM-NK and eUC-NK. (F) KDA analysis of the DEGs (log_2FC >1.0) between eBM-NK and eUC-NK. (G) Variable shear events in eBM-NK and eUC-NK. (H) The distribution of the differentially VSE (DVSE) between eBM-NK and eUC-NK. (I) Circos diagrams revealed the distribution of fusion genes in eBM-NK and eUC-NK.

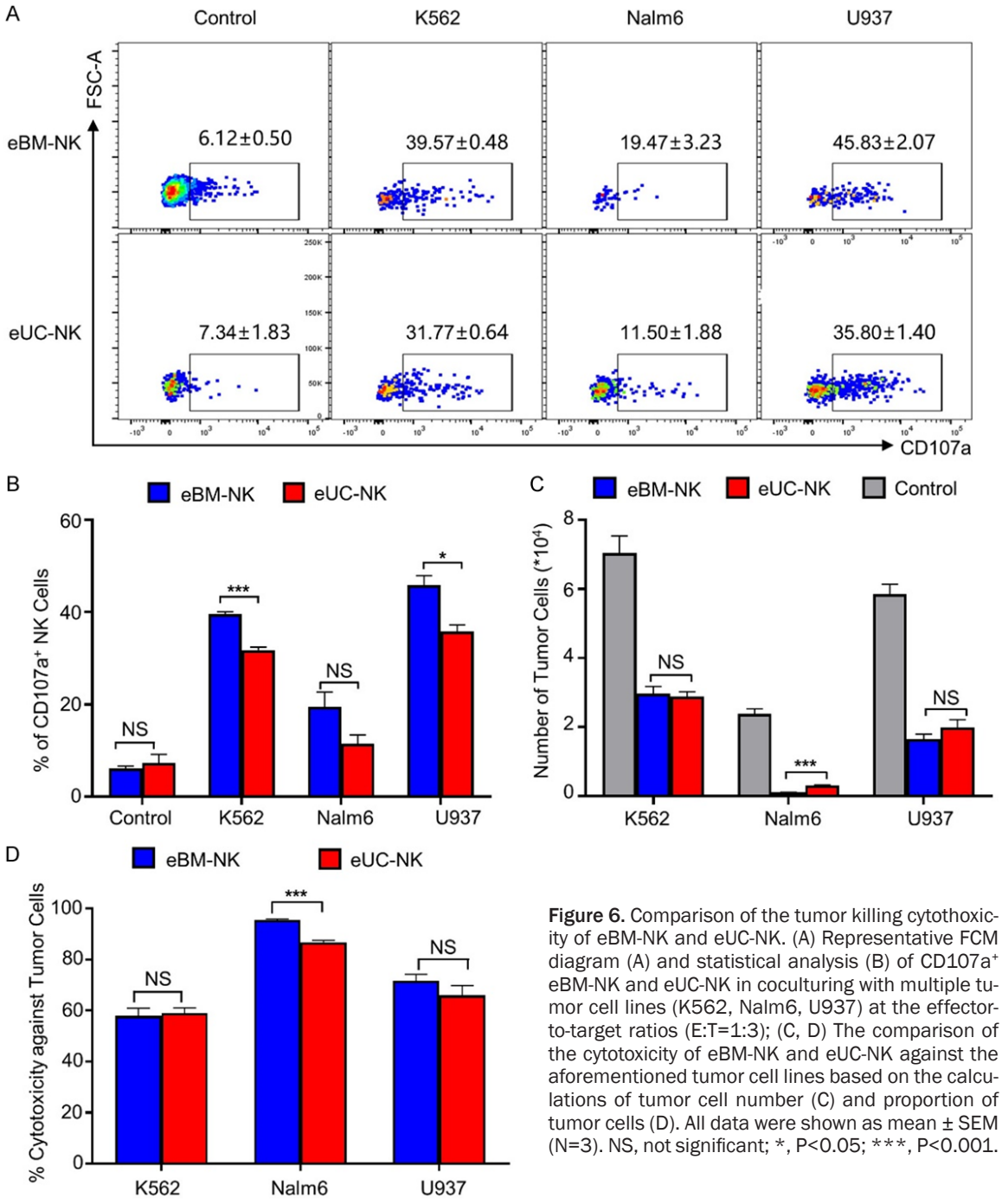

Figure 6. Comparison of the tumor killing cytothoxicity of eBM-NK and eUC-NK. (A) Representative FCM diagram (A) and statistical analysis (B) of CD107a$^+$ eBM-NK and eUC-NK in coculturing with multiple tumor cell lines (K562, Nalm6, U937) at the effector-to-target ratios (E:T=1:3); (C, D) The comparison of the cytotoxicity of eBM-NK and eUC-NK against the aforementioned tumor cell lines based on the calculations of tumor cell number (C) and proportion of tumor cells (D). All data were shown as mean ± SEM (N=3). NS, not significant; *, P<0.05; ***, P<0.001.

CD56$^+$ rNK), coculture with feeder cells (e.g., K562, K562-mbIL2-I L15-IL18-41BBL), cytokine cocktail-initiated programming (e.g., IL-2, IL-7, IL-18, IL-21), cell sorting or magnetic activated cell sorting (MACS), and physicochemical irritation (e.g., bioreactor, culture vessels) [21, 47]. Of note, we verified that the "discarded" perinatal blood including placental blood and umbilical cord blood are preferable alternatives for fulfilling the high-efficient and cost-effective preparation of GMP-grade NK cell products for cancer immunotherapy in future.

NK cells function mainly via antibody-dependent cell-mediated cytotoxicity (ADCC), receptor-ligand related cytotoxicity, secretion of granzyme and perforin, and cytokine-based paracrine effects (e.g., GM-CSF, IFN-γ) [7, 48].

Despite the robust prospective of NK cell-based cancer immunotherapy, yet the large-scale application in clinical practice is still restricted largely attributes to the limitation of alternative sources and cost-effective strategies for preparing NK cells with functional maturation after *ex vivo* "NK cell education" [49]. Meanwhile, the systematic and detailed illumination of NK cells with different origins is simultaneously obscure, which further hinders the development of NK cell-based cytotherapy for cancer immunotherapy. Therefore, depicting the biological signatures and transcriptomic characteristics has been acknowledged to supply basic knowhow for developing and improving novel remedies for cancer management [50, 51]. For the purpose, in this study we verified the multifaceted characterizations of the biological and transcriptomic signatures of eBM-NK and eUC-NK, together with the immunophenotypes of the corresponding rBM-NK and rUC-NK as well. Collectively, our findings suggested umbilical cord blood as preferable alternatives over bone marrow for NK cell-based cancer immunotherapy.

Acknowledgements

We thank all the members in the researcher team of the First Affiliated Hospital of Kunming Medical University for their professional assistance. We also thank Health-Biotech (Tianjin) Stem Cell Research Institute Co., Ltd., the Key Laboratory of Molecular Diagnostics and Precision Medicine for Surgical Oncology in Gansu Province & NHC Key Laboratory of Diagnosis and Therapy of Gastrointestinal Tumor in Gansu Provincial Hospital, School of Basic Medical Sciences in Anhui Medical University, the First Affiliated Hospital of Hainan Medical University, Hefei Institute of Physical Science in Chinese Academy of Sciences, and Chinese Academy of Medical Sciences & Peking Union Medical College for their technical support. The work was supported by National Natural Science Foundation of China (No. 82260031, 8207-2880, 81960283, 82173377 and 81302319), Major Science and Technology Program of Hainan Province (No. ZDKJ2021037, ZDKJ-202003), Jiangxi Provincial leading Talent of "Double Thousand Plan" (2022 to L.S.Z.), Major Research Project of Education Department of Anhui Province (KJ2018ZD018), Key Project funded by Department of Science and Technology of Shangrao City (2020AB002, 2022-A001, 2020K003, 2021F013, 2022AB003), The Famous Medical Specialist of "High-level Talent Training Support Program" in Yunnan Province (RLMY20190004), Yunnan Science and Technology Project (L-2017018), Project of Yunnan Applied Basic Research Project Kunming Medical University Union Foundation (202201AY070001-042), Clinical Research Center for Geriatric Diseases of Yunnan Province - diagnosis and treatment of geriatric comorbidity and clinical translational research (202102AA310069), The Innovative Team of Yunnan Province (202305AS350019), Science and Technology Projects of Guizhou Province (QKH-J-ZK [2021]-107), Natural Science Foundation of Hainan Province (ZDYF2020117), project of Hainan Clinical Research Center (LCYX202102), Natural Science Foundation of Jiangxi Province (20212BAB216073), project supported by Hainan Province Clinical Medical Center (to B.G.X.), Natural Science Foundation of Fujian Province (2022J01266), Joint Major Project of Science and Technology Innovation in Fujian Province (2021Y9083), Gansu Provincial Hospital Intra-Hospital Research Fund Project (22GSSYB-6, 21GSSYB-8, 22GSSYC-20, 20GSSY5-2), The 2022 Master/Doctor/Postdoctoral program of NHC Key Laboratory of Diagnosis and Therapy of Gastrointestinal Tumor (NHCDP2022004, NHCDP2022008, NHCDP2022014, NHCDP20220220), the Non-profit Central Research Institute Fund of Chinese Academy of Medical Sciences (2019-PT320005), The 2021 Central-Guided Local Science and Technology Development Fund (ZYYDDFFZZJ-1), Fujian Provincial Ministerial Finance Special Project (2021XH018), Medical Innovation Project of Fujian Provincial Health and Health Commission (2019-CX-21).

Disclosure of conflict of interest

None.

Abbreviations

UCB, Umbilical cord blood; NK, natural killer; DEGs, differentially expressed genes; HSCs, hematopoietic stem cells; PCA, principal component analysis; FPKM, fragments per kilobase million; VSE, variable shear event; DVSE, differentially variable shear event; PPI, protein-pro-

tein interaction; GSEA, gene set enrichment analysis; KEGG, Kyoto encyclopedia of genes and genomes; GOBP, gene ontology biological process; TPM, transcripts per kilobase of exon model per million mapped reads; MNCs, mononuclear cells; rNK, resident natural killer cells; eNK, expanded natural killer cells; rBM-NK, resident NK cells in bone marrow-derived MNCs.

Address correspondence to: Dr. Cunrong Chen, Department of Critical Care Medicine, Fujian Medical University Union Hospital, Fuzhou 350001, Fujian, China. E-mail: 13705056799@139.com; Dr. Feifei Li, Department of Pathophysiology, School of Basic Medical Sciences, Anhui Medical University, Hefei 230032, Anhui, China. E-mail: Feifei.Li@ahmu.edu.cn; Dr. Yihu Fang, Institute of Stem Cell, Jiangxi Medical College, Shangrao 334000, Jiangxi, China. E-mail: joan0920@163.com; Dr. Hongju Yang, Division of Gastroenterology, The First Affiliated Hospital of Kunming Medical University, Kunming 650031, Yunnan, China. E-mail: hongjuyang105@163.com

References

[1] Siegel RL, Miller KD, Fuchs HE and Jemal A. Cancer statistics, 2021. CA Cancer J Clin 2021; 71: 7-33.

[2] Siegel RL, Miller KD and Jemal A. Cancer statistics, 2020. CA Cancer J Clin 2020; 70: 7-30.

[3] Wang Y, Liu T, Li X, Sheng H, Ma X and Hao L. Ferroptosis-inducing nanomedicine for cancer therapy. Front Pharmacol 2021; 12: 735965.

[4] Walcher L, Kistenmacher AK, Suo H, Kitte R, Dluczek S, Strauß A, Blaudszun AR, Yevsa T, Fricke S and Kossatz-Boehlert U. Cancer stem cells-origins and biomarkers: perspectives for targeted personalized therapies. Front Immunol 2020; 11: 1280.

[5] Siegel RL, Miller KD, Fuchs HE and Jemal A. Cancer statistics, 2022. CA Cancer J Clin 2022; 72: 7-33.

[6] Anand S, Chan TA, Hasan T and Maytin EV. Current prospects for treatment of solid tumors via photodynamic, photothermal, or ionizing radiation therapies combined with immune checkpoint inhibition (a review). Pharmaceuticals (Basel) 2021; 14: 447.

[7] Zhang L, Liu M, Yang S, Wang J, Feng X and Han Z. Natural killer cells: of-the-shelf cytotherapy for cancer immunosurveillance. Am J Cancer Res 2021; 11: 1770-1791.

[8] Depil S, Duchateau P, Grupp SA, Mufti G and Poirot L. 'Off-the-shelf' allogeneic CAR T cells: development and challenges. Nat Rev Drug Discov 2020; 19: 185-199.

[9] Chen M, Hu S, Li Y, Jiang TT, Jin H and Feng L. Targeting nuclear acid-mediated immunity in cancer immune checkpoint inhibitor therapies. Signal Transduct Target Ther 2020; 5: 270.

[10] Solaini L, Perna F, Cavaliere D, Vaccaro C, Avanzolini A, Cucchetti A, Coratti A and Ercolani G. Average treatment effect of robotic versus laparoscopic rectal surgery for rectal cancer. Int J Med Robot 2021; 17: e2210.

[11] Ang MJY, Chan SY, Goh YY, Luo Z, Lau JW and Liu X. Emerging strategies in developing multifunctional nanomaterials for cancer nanotheranostics. Adv Drug Deliv Rev 2021; 178: 113907.

[12] Zhang L, Meng Y, Feng X and Han Z. CAR-NK cells for cancer immunotherapy: from bench to bedside. Biomark Res 2022; 10: 12.

[13] Kennedy LB and Salama AKS. A review of cancer immunotherapy toxicity. CA Cancer J Clin 2020; 70: 86-104.

[14] Childs RW and Carlsten M. Therapeutic approaches to enhance natural killer cell cytotoxicity against cancer: the force awakens. Nat Rev Drug Discov 2015; 14: 487-498.

[15] Siegler EL, Zhu Y, Wang P and Yang L. Off-the-shelf CAR-NK cells for cancer immunotherapy. Cell Stem Cell 2018; 23: 160-161.

[16] Daher M, Melo Garcia L, Li Y and Rezvani K. CAR-NK cells: the next wave of cellular therapy for cancer. Clin Transl Immunology 2021; 10: e1274.

[17] Wu F, Xie M, Hun M, She Z, Li C, Luo S, Chen X, Wan W, Wen C and Tian J. Natural killer cell-derived extracellular vesicles: novel players in cancer immunotherapy. Front Immunol 2021; 12: 658698.

[18] Xie G, Dong H, Liang Y, Ham JD, Rizwan R and Chen J. CAR-NK cells: a promising cellular immunotherapy for cancer. EBioMedicine 2020; 59: 102975.

[19] Liu M, Meng Y, Zhang L, Han Z and Feng X. High-efficient generation of natural killer cells from peripheral blood with preferable cell vitality and enhanced cytotoxicity by combination of IL-2, IL-15 and IL-18. Biochem Biophys Res Commun 2021; 534: 149-156.

[20] Zhang L, Liu M, Song B, Miao W, Zhan R, Yang S, Han Z, Cai H, Xu X, Zhao Y, Han Z, Guo T, Yao J and Huang Q. Decoding the multidimensional signatures of resident and expanded natural killer cells generated from perinatal blood. Am J Cancer Res 2022; 12: 2132-2145.

[21] Gao H, Liu M, Zhang Y, Zhang L and Xie B. Multifaceted characterization of the biological and transcriptomic signatures of natural killer cells derived from cord blood and placental blood. Cancer Cell Int 2022; 22: 291.

[22] Nair S, Fang M and Sigal LJ. The natural killer cell dysfunction of aged mice is due to the

bone marrow stroma and is not restored by IL-15/IL-15Ralpha treatment. Aging Cell 2015; 14: 180-190.

[23] Shah N, Martin-Antonio B, Yang H, Ku S, Lee DA, Cooper LJ, Decker WK, Li S, Robinson SN, Sekine T, Parmar S, Gribben J, Wang M, Rezvani K, Yvon E, Najjar A, Burks J, Kaur I, Champlin RE, Bollard CM and Shpall EJ. Antigen presenting cell-mediated expansion of human umbilical cord blood yields log-scale expansion of natural killer cells with anti-myeloma activity. PLoS One 2013; 8: e76781.

[24] Kang L, Voskinarian-Berse V, Law E, Reddin T, Bhatia M, Hariri A, Ning Y, Dong D, Maguire T, Yarmush M, Hofgartner W, Abbot S, Zhang X and Hariri R. Characterization and ex vivo expansion of human placenta-derived natural killer cells for cancer immunotherapy. Front Immunol 2013; 4: 101.

[25] Wei Y, Zhang L, Chi Y, Ren X, Gao Y, Song B, Li C, Han Z, Zhang L and Han Z. High-efficient generation of VCAM-1(+) mesenchymal stem cells with multidimensional superiorities in signatures and efficacy on aplastic anaemia mice. Cell Prolif 2020; 53: e12862.

[26] Zhang L, Wei Y, Chi Y, Liu D, Yang S, Han Z and Li Z. Two-step generation of mesenchymal stem/stromal cells from human pluripotent stem cells with reinforced efficacy upon osteoarthritis rabbits by HA hydrogel. Cell Biosci 2021; 11: 6.

[27] Zhang L, Chi Y, Wei Y, Zhang W, Wang F, Zhang L, Zou L, Song B, Zhao X and Han Z. Bone marrow-derived mesenchymal stem/stromal cells in patients with acute myeloid leukemia reveal transcriptome alterations and deficiency in cellular vitality. Stem Cell Res Ther 2021; 12: 365.

[28] Zhang L, Wang H, Liu C, Wu Q, Su P, Wu D, Guo J, Zhou W, Xu Y, Shi L and Zhou J. MSX2 initiates and accelerates mesenchymal stem/stromal cell specification of hPSCs by regulating TWIST1 and PRAME. Stem Cell Reports 2018; 11: 497-513.

[29] Zhang L, Zou L, Ma Y, Feng C, Zhan R, Yang H, Song B and Han Z. Multifaceted modifications for a cell size-based circulating tumor cell scope technique hold the prospect for large-scale application in general populations. Cell Biol Int 2021; 45: 345-357.

[30] Zhang L, Liu C, Wang H, Wu D, Su P, Wang M, Guo J, Zhao S, Dong S, Zhou W, Arakaki C, Zhang X and Zhou J. Thrombopoietin knock-in augments platelet generation from human embryonic stem cells. Stem Cell Res Ther 2018; 9: 194.

[31] Zhang W, Liu C, Wu D, Liang C, Zhang L, Zhang Q, Liu Y, Xia M, Wang H, Su P, Feng S, Han M, Zhou J, Wang F and Jiang E. Decitabine improves platelet recovery by down-regulating IL-8 level in MDS/AML patients with thrombocytopenia. Blood Cells Mol Dis 2019; 76: 66-71.

[32] Holyoake DLP and Smyth EC. Chemoradiotherapy or surgery for very early esophageal squamous cancer: can a nonrandomized trial give us the answer? Gastroenterology 2021; 161: 1793-1795.

[33] Bordon Y. An RNA vaccine for advanced melanoma. Nat Rev Immunol 2020; 20: 517.

[34] Sahin U, Oehm P, Derhovanessian E, Jabulowsky RA, Vormehr M, Gold M, Maurus D, Schwarck-Kokarakis D, Kuhn AN, Omokoko T, Kranz LM, Diken M, Kreiter S, Haas H, Attig S, Rae R, Cuk K, Kemmer-Bruck A, Breitkreuz A, Tolliver C, Caspar J, Quinkhardt J, Hebich L, Stein M, Hohberger A, Vogler I, Liebig I, Renken S, Sikorski J, Leierer M, Muller V, Mitzel-Rink H, Miederer M, Huber C, Grabbe S, Utikal J, Pinter A, Kaufmann R, Hassel JC, Loquai C and Tureci O. An RNA vaccine drives immunity in checkpoint-inhibitor-treated melanoma. Nature 2020; 585: 107-112.

[35] Rohatgi A and Kirkwood JM. Cancer vaccine induces potent T cell responses - but is it enough? Nat Rev Clin Oncol 2020; 17: 721-722.

[36] Sahin U, Derhovanessian E, Miller M, Kloke BP, Simon P, Lower M, Bukur V, Tadmor AD, Luxemburger U, Schrors B, Omokoko T, Vormehr M, Albrecht C, Paruzynski A, Kuhn AN, Buck J, Heesch S, Schreeb KH, Muller F, Ortseifer I, Vogler I, Godehardt E, Attig S, Rae R, Breitkreuz A, Tolliver C, Suchan M, Martic G, Hohberger A, Sorn P, Diekmann J, Ciesla J, Waksmann O, Bruck AK, Witt M, Zillgen M, Rothermel A, Kasemann B, Langer D, Bolte S, Diken M, Kreiter S, Nemecek R, Gebhardt C, Grabbe S, Holler C, Utikal J, Huber C, Loquai C and Tureci O. Personalized RNA mutanome vaccines mobilize poly-specific therapeutic immunity against cancer. Nature 2017; 547: 222-226.

[37] Pan J, Niu Q, Deng B, Liu S, Wu T, Gao Z, Liu Z, Zhang Y, Qu X, Zhang Y, Liu S, Ling Z, Lin Y, Zhao Y, Song Y, Tan X, Zhang Y, Li Z, Yin Z, Chen B, Yu X, Yan J, Zheng Q, Zhou X, Gao J, Chang AH, Feng X and Tong C. CD22 CAR T-cell therapy in refractory or relapsed B acute lymphoblastic leukemia. Leukemia 2019; 33: 2854-2866.

[38] Pan J, Zuo S, Deng B, Xu X, Li C, Zheng Q, Ling Z, Song W, Xu J, Duan J, Wang Z, Yu X, Chang AH, Feng X and Tong C. Sequential CD19-22 CAR T therapy induces sustained remission in children with r/r B-ALL. Blood 2020; 135: 387-391.

[39] Pan J, Tan Y, Deng B, Tong C, Hua L, Ling Z, Song W, Xu J, Duan J, Wang Z, Guo H, Yu X,

Chang AH, Zheng Q and Feng X. Frequent occurrence of CD19-negative relapse after CD19 CAR T and consolidation therapy in 14 TP53-mutated r/r B-ALL children. Leukemia 2020; 34: 3382-3387.
[40] Roselli E, Faramand R and Davila ML. Insight into next-generation CAR therapeutics: designing CAR T cells to improve clinical outcomes. J Clin Invest 2021; 131: e142030.
[41] Frigault MJ and Maus MV. State of the art in CAR T cell therapy for CD19+ B cell malignancies. J Clin Invest 2020; 130: 1586-1594.
[42] Li D, Li X, Zhou WL, Huang Y, Liang X, Jiang L, Yang X, Sun J, Li Z, Han WD and Wang W. Genetically engineered T cells for cancer immunotherapy. Signal Transduct Target Ther 2019; 4: 35.
[43] Marofi F, Rahman HS, Thangavelu L, Dorofeev A, Bayas-Morejon F, Shirafkan N, Shomali N, Chartrand MS, Jarahian M, Vahedi G, Mohammed RN, Shahrokh S, Akbari M and Khiavi FM. Renaissance of armored immune effector cells, CAR-NK cells, brings the higher hope for successful cancer therapy. Stem Cell Res Ther 2021; 12: 200.
[44] Berrien-Elliott MM, Cashen AF, Cubitt CC, Neal CC, Wong P, Wagner JA, Foster M, Schappe T, Desai S, McClain E, Becker-Hapak M, Foltz JA, Cooper ML, Jaeger N, Srivatsan SN, Gao F, Romee R, Abboud CN, Uy GL, Westervelt P, Jacoby MA, Pusic I, Stockerl-Goldstein KE, Schroeder MA, DiPersio J and Fehniger TA. Multidimensional analyses of donor memory-like NK cells reveal new associations with response after adoptive immunotherapy for leukemia. Cancer Discov 2020; 10: 1854-1871.
[45] Basar R, Daher M and Rezvani K. Next-generation cell therapies: the emerging role of CAR-NK cells. Blood Adv 2020; 4: 5868-5876.
[46] Wrona E, Borowiec M and Potemski P. CAR-NK cells in the treatment of solid tumors. Int J Mol Sci 2021; 22: 5899.
[47] Guillerey C, Huntington ND and Smyth MJ. Targeting natural killer cells in cancer immunotherapy. Nat Immunol 2016; 17: 1025-1036.
[48] Bryceson YT, March ME, Ljunggren HG and Long EO. Activation, coactivation, and costimulation of resting human natural killer cells. Immunol Rev 2006; 214: 73-91.
[49] Vivier E. What is natural in natural killer cells? Immunol Lett 2006; 107: 1-7.
[50] Feng RM, Zong YN, Cao SM and Xu RH. Current cancer situation in China: good or bad news from the 2018 global cancer statistics? Cancer Commun (Lond) 2019; 39: 22.
[51] Wei W, Zeng H, Zheng R, Zhang S, An L, Chen R, Wang S, Sun K, Matsuda T, Bray F and He J. Cancer registration in China and its role in cancer prevention and control. Lancet Oncol 2020; 21: e342-e349.

Supplementary Table 1. The list of the cytokines

Reagent	Cat. No.	Conc.	Source
Recombinant Human IL-2 (rhIL-2)	200-02	100 ng/uL	PeproTech Inc, USA
Recombinant Human IL-15 (rhIL-15)	200-15	10 ng/uL	PeproTech Inc, USA
Recombinant Human IL-18 (rhIL-18)	119-BP-100	10 ng/uL	R&D Systems, USA

Supplementary Table 2. The list of the antibodies

Antibody	Cat. No.	Source
Anti-CD3-PE	981004	BioLegend
Anti-CD3-APC-Cy7	300316	BioLegend
Anti-CD4-PE	357403	BioLegend
Anti-CD8-PE-Cy7	344711	BioLegend
Anti-CD16-FITC	302005	BioLegend
Anti-NKG2D-Percp-cy5.5	320817	BioLegend
Anti-CD56-APC	362503	BioLegend
Anti-CD56-Percp-cy5.5	362505	BioLegend
Anti-CD107a-PE-Cy7	328617	BioLegend
7-AAD-Percp-cy5.5	559925	BD Pharmigen
PE anti-human IgG	409304	BioLegend
Percision Count Beads	424902	BioLegend
DAPI	MBD0015	Sigma-Aldrich
Cell Cycle and Apoptosis Detection Kit	C1052	Beyotime Biotehnology
CellTrace Voilet	C34557	Invitrogen™
Annexin V-FITC	AO2001-02G	Tianjin Sungene Biotech
Annexin V binding buffer (10X)	AB2000-G	Tianjin Sungene Biotech